International Journal of Geographical Information Science, 2015
http://dx.doi.org/10.1080/13658816.2015.1009911

Taylor & Francis
Taylor & Francis Group

Improving the representation of major landforms in analytical relief shading

Brooke E. Marston* and Bernhard Jenny

College of Earth, Ocean, and Atmospheric Sciences, Oregon State University, Corvallis, OR, USA

(*Received 12 September 2014; final version received 17 December 2014*)

Relief shading is the most common type of cartographic relief representation for print and digital maps. Manual relief shading results in informative and visually pleasing representations of terrain, but it is time consuming and expensive to produce. Current analytical relief shading can be created quickly, but the resulting maps are not as aesthetically appealing and do not show landscape features in an explicit manner. This article introduces an automated digital method that produces shaded relief with locally adjusted illumination directions to simulate the techniques and cartographic principles of manual relief shading. Ridgelines and valley lines are derived from a digital terrain model, vectorized, and used in a diffusion curve algorithm. A graph analysis generalizes the lines before using them for diffusion curve shading. The direction of illumination is adjusted based on the spatial orientation of ridgelines and valley lines. The diffusion curve shading is combined with standard analytical relief shading to create a final diffusion relief shading image. Similar to manual relief shading, major landforms and the structure of the terrain are more clearly shown in the diffusion relief shading. The presented method best highlights major landforms in terrain characterized by sharp, clearly defined ridges and valleys.

Keywords: terrain mapping; diffusion curves; relief shading; shaded relief; hill shading; Swiss-style; diffusion relief shading

1. Introduction

Relief shading is a cartographic technique used to depict topography by applying a virtual illumination source to terrain. The resulting distribution of light and shadows provides a three-dimensional configuration of the terrain's geomorphological structure that imitates the natural appearance of landscapes. Unlike contour lines, which allow users to interpolate terrain elevations, relief shading relies on varying continuous shading tones to depict the topographic surface form in a more intuitive manner. Contour lines typically require careful analysis to determine surface forms and properties and may prove challenging to interpret. Quick comprehension of surface topography is an inherent appeal of relief shading. As a result, relief shading is preferable for users with little or no cartographic training or with limited time to interpret terrain. Relief shading is also beneficial for small-scale maps where traditional contour lines may be indistinguishable or unreadable (Imhof 1982).

Historically, relief shading was produced by manual methods. Contour lines, geomorphological structure lines, and hydrographic networks served as a framework for

*Corresponding author. Email: marstonb@onid.orst.edu

designing shaded relief. A thorough understanding of the landscape was required for cartographers to translate topography into artistic maps. Cartographers have developed design principles for manual relief shading that make legible, descriptive, and visually pleasing relief representations where major landform systems and detailed features of the terrain are both shown. Important topographic features are emphasized by locally adjusting the direction of illumination according to a feature's spatial orientation. Locally shaded and illuminated slopes help users to better perceive major landforms and improve the aesthetic quality of a map.

Since the 1960s, relief shading has been derived analytically from computer calculations based on digital terrain models. However, current analytical relief shading largely ignores the traditional cartographic techniques developed for manual relief shading. One of the most distinct differences between manual and analytical relief shading is that the direction of illumination is generally not adjusted to highlight select terrain features in analytical shading. In analytical shading, a single direction of illumination often does not produce shaded relief images that effectively portray terrain in an appealing manner. Generally, cartographers prefer the legibility and aesthetic quality of well-executed manual relief shading to analytical relief shading (Jenny 2001). However, cartographers who seek to adjust the direction of illumination in analytical shading are required to do a considerable amount of work to produce a desirable result.

Automating the cartographic principles and techniques associated with traditional manual relief shading, but in a computerized environment, is beneficial for several reasons: (1) shaded relief adhering to manual design principles can be produced more quickly than current methods allow; (2) more aesthetically pleasing maps can be produced; (3) major landforms can be shown more explicitly, making it easier and faster for the user to achieve an overall sense of landform structure, while maintaining the ability to discern important small details; and (4) techniques and tools used to improve the quality of maps can be made available to all mapmakers. This article presents a new digital method to highlight major landforms, as inspired by manual techniques for relief representation, in analytical shading using diffusion curves, which were developed in computer graphics to create images with smooth color gradients. Ridgelines and valley lines are extracted from a digital terrain model and used in a diffusion curve algorithm to create a shading image. The extracted ridgelines and valley lines are used to identify major landforms, which are scale dependent. A graph analysis generalizes the ridgeline geometry, which, along with the valley line geometry, is used to adjust the direction of illumination. The diffusion relief shading, a combination of the diffusion curve shading and analytical relief shading, simulates the design characteristics of manual relief shading.

2. Literature review

2.1. Manual relief shading

The standard direction of illumination in relief shading is from the northwest. Northwest illumination is preferred by most users, who have become accustomed to lighting from above and to the left, supposedly a consequence of left-to-right writing and drawing techniques (Imhof 1982). In manual relief shading, illumination is locally altered to make an effective visual image intuitive for readers (Yoeli 1959, Brassel 1974, Imhof 1982, Karssen 1982, Jenny 2001, Hurni 2008). Specially trained cartographers carefully analyze

landscapes to determine prominent terrain features to highlight while simultaneously minimizing the visual impact of uninteresting or excessive detail in the terrain.

The style of relief depiction developed by Swiss cartographers is highly acclaimed for its beauty and detail (Tufte 1990, Kennelly and Stewart 2006) and can be regarded as the foremost exemplary model for relief representation (Hodgkiss 1981, Knowles and Stowe 1982, Keates 1996, Collier *et al.* 2003, Jenny *et al.* 2010). Among the pioneers in Swiss mountain cartography are Rudolf Leuzinger (1826–1896), who created the first colored relief maps for the Swiss Alpine Club in 1863 (Jenny and Hurni 2006), Fridolin Becker (1854–1922), and Eduard Imhof (1895–1986). Becker improved Leuzinger's method by developing a more natural color depiction (Hurni 2008) and perfected the simulation of the aerial perspective effect in printed maps by sharpening contrast in the highest peaks (Jenny and Hurni 2006). Imhof refined and standardized Becker's design principles to form the foundation for exquisite map design exemplified by the 1963 'Graubünden' map (Figure 1).

The principles of Swiss-style relief shading for an informative and explicit portrayal of terrain as described by Imhof (1982) are (1) local adjustments of the illumination source to

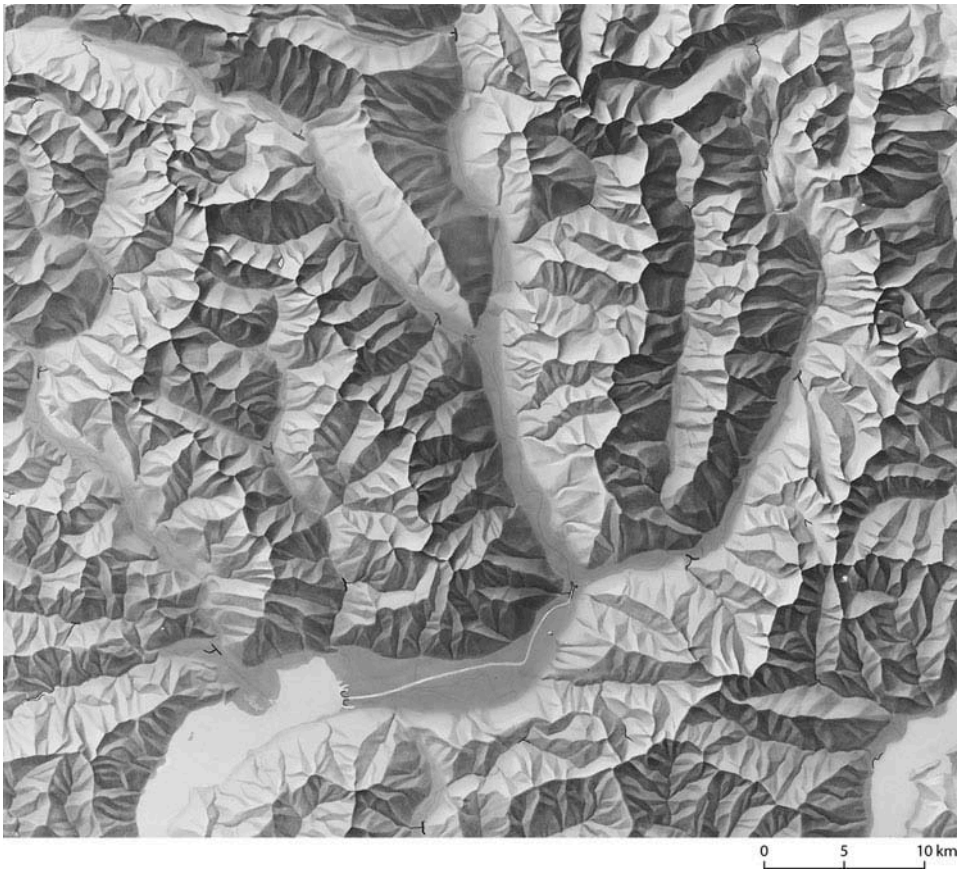

Figure 1. Ticino section of 'Graubünden' (Canton of Grisons). By E. Imhof and H. Leuzinger, 1963 (from shadedreliefarchive.com).

emphasize select topographic features; (2) bright gray tones placed in flat areas to visually connect adjacent hillslopes; (3) brightness adjustments on illuminated and shadowed slopes; and (4) inclusion of aerial perspective to distinguish between the highest mountain peaks and lowlands.

2.2. *Analytical relief shading*

Analytical relief shading is the computer-based process of deriving a shaded relief from a digital terrain model. Shaded relief consists of gray values stored in raster images. Wiechel (1878) proposed a mathematical approach to analytical relief shading based on Lambert's law of cosines in the late 1800s, but it was not implemented until the mid-twentieth century due to insufficient computing facilities. In the 1960s, Yoeli produced the first analytical relief shading by applying Wiechel's method (Yoeli 1965, 1966). The Lambert shading algorithm, the fundamental of most analytically shaded models used in geographic information systems, determines the gray value for each pixel by calculating the angle between a virtual illumination and the surface normal (Yoeli 1965).

While manual relief shading is an arduous, time-intensive task, analytical relief shading is faster and less expensive to produce than manual relief shading. However, standard analytical shading does not create an aesthetically pleasing image adhering to principles developed for manual relief shading. In manual relief shading, the direction of illumination is generally adjusted locally to the characteristics of certain landforms; however, in analytical shading, there is a global direction of illumination that is not typically adjusted (Figure 2). Since Yoeli's attempt at analytical relief shading, numerous other methods for analytical shading have been

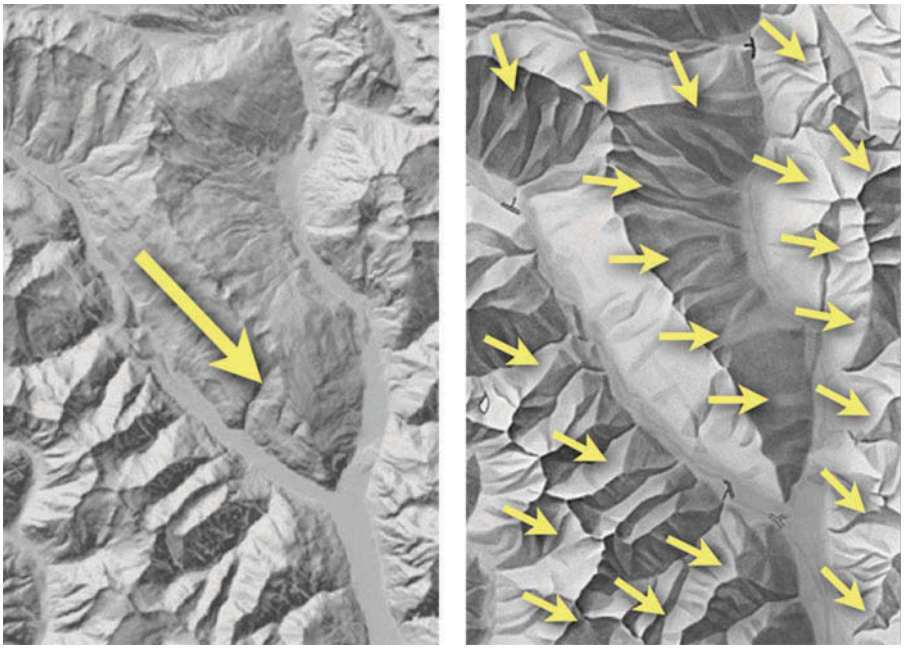

Figure 2. Analytical shading with one direction of illumination (left) and manual shading with multiple combined illumination directions (right). The manually adjusted illumination shows landforms more clearly.

developed to simulate the complex process of manual shading. Combining multiple illumination directions to simulate the local adjustment of illumination (Yoeli 1967, Brassel 1974, Mark 1992, Hobbs 1999, Jenny 2001, Kennelly and Stewart 2006, Loisios *et al.* 2007, Veronesi and Hurni 2014) (Figure 2) and using curvature to enhance topographic detail (Kennelly 2008, Leonowicz *et al.* 2010a, 2010b) are techniques cartographers use to imitate manual relief shading. The application of aerial perspective (Brassel 1974, Jenny 2001), vertical exaggeration (Patterson and Hermann 2004), and terrain generalization to remove unwanted detail and accentuate important landforms (Weibel 1992, Prechtel 2000, Patterson 2001, Leonowicz *et al.* 2010a, 2010b) has also been attempted to improve analytical relief shading.

3. Methods

3.1. Overview of method

A diffusion curve algorithm renders a shaded image defined by a set of terrain skeletal lines (Imhof 1982) – valley lines and ridgelines – extracted from a terrain model. Valley lines are identified in a digital terrain model using a flow accumulation method. Ridgelines are identified by maximum branch length. We extend the maximum branch length method to remove irrelevant ridgelines by tilting the digital terrain model in the primary cardinal and intercardinal directions. We vectorize the ridgelines and valley lines and implement a graph analysis to generalize the ridgelines. The direction of illumination is adjusted based on the spatial orientation of the skeletal lines. We use a seed fill algorithm to detect and mask flat areas, such as the valley floor, in the terrain. The diffusion curve shading is combined with the analytical relief shading and valley floor mask to produce a final relief image. Figure 3 provides a comprehensive overview of our procedure.

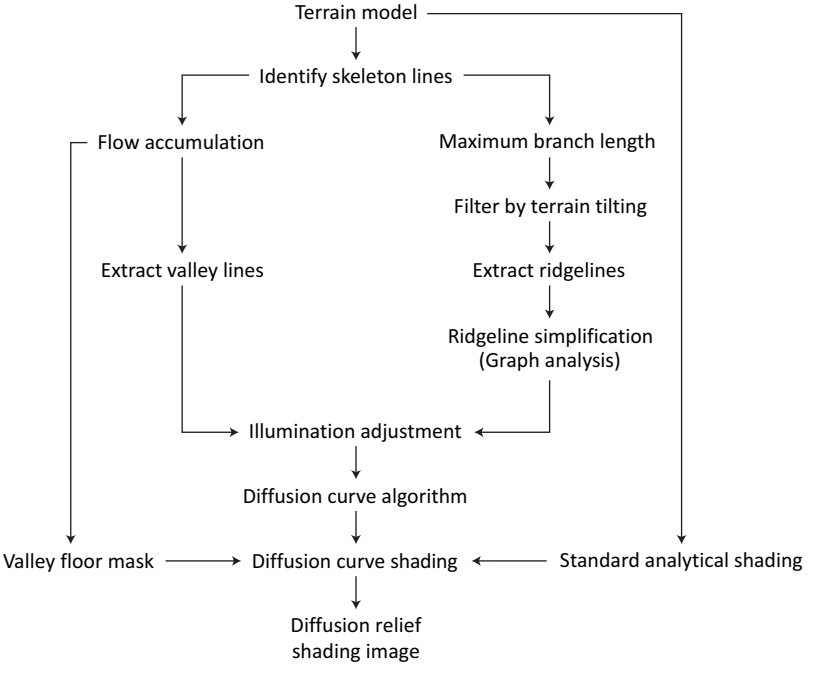

Figure 3. Processing steps for creating a diffusion relief shading image.

The different processes applied in our method are explained in the following sections. We first introduce diffusion curves (Section 3.2) and describe the identification of terrain skeletal lines (Section 3.3) and the terrain tilting procedure for filtering irrelevant ridgelines (Section 3.4). Next, we discuss vectorizing skeletal lines (Section 3.5), generalizing ridgelines by graph analysis (Section 3.6), the local adjustment of illumination directions based on skeletal lines (Section 3.7), and the identification of valley floors (Section 3.8). Finally, we describe the combination of different software and implementation details (Section 3.9).

3.2. *Diffusion curves*

Diffusion curves, introduced by Orzan *et al.* (2008), create images with smooth color gradients. Orzan *et al.* vectorized edges to allow for manipulation of shape, color, contrast, and blur values. The diffusion curve developed by Orzan *et al.* is a cubic Bézier spline, specified by control points, that divides a two-dimensional space. Diffusion curves are defined with two parameters, color and blur, which may vary along the curve. Linear interpolation is used to diffuse colors independently on the left and right sides of the curve outward to fill the image plane (Figure 4). The blur attribute controls the smoothness of the transition between the two sides. Rendering an image with Orzan *et al.*'s technique involves three steps: (1) computing color source and gradient fields and rasterizing the continuous curves into a discrete image; (2) solving a Poisson equation with a GPU implementation; and (3) blurring the color image, produced by the diffusion process, according to a blur map derived from blur values stored along each curve.

There are several limitations to Orzan *et al.*'s method. Applying the blur map averages the colors in the image so that the colors along the curve no longer match the color specified by the user. The algorithm that renders the diffusion curves can create artifacts such as color bleeding. Jeschke *et al.* (2009) use a diffusion solver with variable stencil sizes to address the limitations of Orzan *et al.*'s method. The alternative, faster blur technique by Jeschke *et al.* (2009) enhances the rasterizing process and improves visual quality.

Improvements continue to be made to the diffusion curve method by extending the work of Orzan *et al.* and Jeschke *et al.* (2009). For example, Bezerra *et al.* (2010) developed directional diffusion and diffusion barrier curves that blocked unwanted colors from diffusing to the other side of a curve, and gave the user more control over the strength of each color in the diffusion process. Rendering quality and performance has been improved (van de Gronde 2010, Boyé *et al.* 2012). Jeschke *et al.* (2011) incorporated texture details and set color constraints to more closely imitate the source image. Finch *et al.* (2011) introduced biharmonic diffusion curves, which control the gradient across a

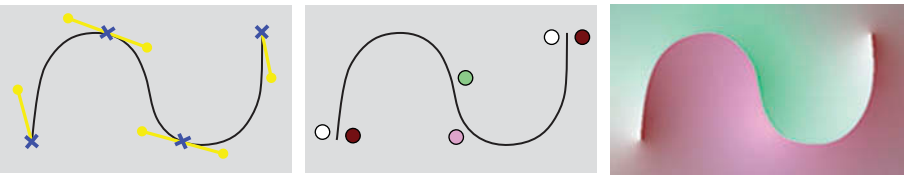

Figure 4. Diffusion curves. Bézier spline with control points (left); colors applied to either side of the curve (center); final image rendered by color diffusion (right).

curve. Additional curve types, including compound curves, have also been developed (Finch *et al.* 2011).

Geisthövel (2013) presented the concept of using diffusion curves for relief shading, but for his shading example, diffusion curves were placed with vector drawing software and were not automatically derived from a digital terrain model. In our method, the diffusion curves represent ridgelines and valley lines. The colors applied to the left and right sides of the curves are grayscale values representing the brightness of the illuminated and shadowed slopes.

3.3. *Identifying terrain skeletal lines*

3.3.1. *Valley line identification*

Valley lines are identified from a terrain model using a flow accumulation method that calculates the accumulated flow into each downslope cell from a flow pointer grid. The flow pointer grid, created by a single-flow-direction algorithm, is generated from a terrain model that has had topographic depressions filled. In our method, we use the deterministic eight-node (D8) algorithm (O'Callaghan and Mark 1984), which is the primary algorithm used to calculate flow pointer grids due to its simplicity and ability to sufficiently delineate catchment boundaries (Wilson and Gallant 2000). The D8 grid indicates primary flow direction by computing flow direction from each cell to a neighboring cell that has the steepest downward gradient. Although alternative algorithms may generate more precise outputs, results from the D8 grid are sufficient for our purposes and produce accurate diffusion curve shading. Additionally, because a mask representing the valley floor is overlaid on top of the diffusion relief shading image and covers the valley lines, precise valley lines are not necessary. Flow accumulation, which is calculated from the D8 grid, can be used to identify a channel by locating areas of concentrated flow. The output of the flow accumulation method is a grid (Figure 5a).

3.3.2. *Ridgeline identification*

Ridgelines are identified using maximum branch length, a topographic attribute conceived by Lindsay and Seibert (2013) to recognize and assess drainage divide network

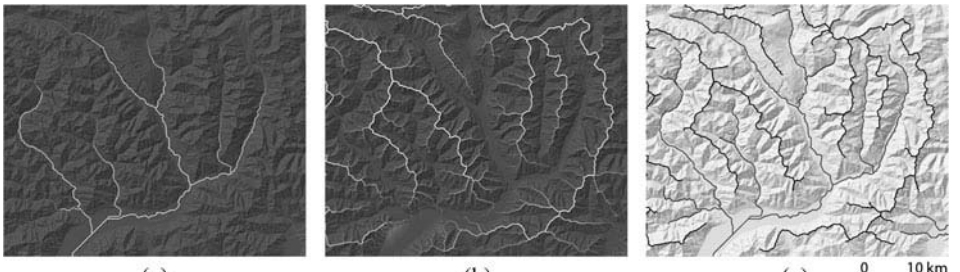

Figure 5. Identification and extraction of terrain skeletal lines. (a) Flow accumulation grid identifying valley lines; (b) maximum branch length grid identifying ridgelines; and (c) vectorized ridgelines (black) and valley lines (gray). All three images are overlaid on top of a standard analytical relief shading. The flow accumulation and maximum branch length grids have been given a slight transparency.

structures in landscapes dissected by river systems. Maximum branch length measures the relative size and significance of drainage divides according to the distance of separation of flow pathways. Lindsay and Seibert define maximum branch length as the maximum distance traveled along a flow path initiated from a grid cell in the terrain model to the confluence with a flow path initiated at a neighboring cell. Because locations along drainage divides are furthest from their downslope confluences, maximum branch length values assigned at divides are several orders of magnitude larger than values assigned along hillslopes. The input for the maximum branch length algorithm is a flow pointer grid generated from a terrain model with filled depressions. The output from the maximum branch length algorithm is a grid (Figure 5b).

3.4. *Filtering ridgelines by terrain tilting*

A limitation of the maximum branch length algorithm is the identification of irrelevant ridgelines, especially in relatively flat terrain. For example, large valleys that have diverging drainage directions prove problematic for creating accurate diffusion curve shading because they produce hard boundaries with sharp contrast in flat areas or in terrain characterized by rounded hills. Although the boundaries are correct in a hydrologic sense, they are unnecessary and result in visually disturbing and confusing shaded relief when used in the diffusion curve algorithm. We remove unnecessary ridgelines with a tilting and filtering process that tests ridgeline stability.

A wedge-shaped base with a user-specified artificial elevation grade (γ in Figure 6) is applied to a terrain model eight times to tilt the terrain model in each of the four cardinal directions – north, south, east, and west – and the four intermediate directions – northeast, northwest, southeast, and southwest. Eight new terrain models are produced with (1) north-south, (2) south-north, (3) east-west, (4) west-east, (5) northwest-southeast, (6) southeast-northwest, (7) southwest-northeast, and (8) northeast-southwest inclinations. For each tilted terrain model, depressions are filled and maximum branch length grids are computed. Figure 6 shows an example of the tilting process for two directions.

Ridgelines are filtered based on their stability throughout the tilting process. Stable ridgelines, a feature of well-defined ridges, experience minimal shifting when the terrain model is tilted (Figure 6). Stable ridgelines are a common trait of sharply defined ridges and are desirable for locally adjusting the illumination

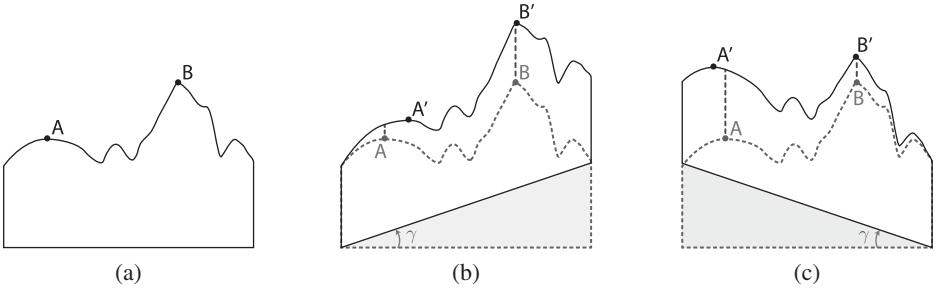

Figure 6. Tilting process to test ridgeline stability. Point A is the ridge of a rounded hill and point B is the ridge of a sharply defined mountain peak. (a) The original terrain model; (b) and (c) are terrain models tilted in opposite directions. In (b) and (c), point A experiences a larger shift in location than point B when comparing the non-tilted and tilted terrain models.

direction for diffusion curve shading. Ridgelines that shift excessively between tiltings are unstable and should be excluded. These ridgelines, where a large contrast in shadowed and illuminated slopes is undesirable, are mostly associated with weakly defined ridges, rounded hills, flat areas, or valleys with multiple drainage directions. The degree of shifting that occurs throughout the tilting process is illustrated for a sample set of ridgelines in Figure 7. To filter out the problematic ridgelines, the amount of shifting a ridgeline experiences throughout the tilting process is detected. The maximum branch length grids are converted to binary grids by thresholding. The eight binary grids are summed together so that the cells in the combined binary grid have a value between 0 and 8. A cell with a value of 0 contains no ridgeline in any of the grids, while a cell value of 8 represents a cell with a ridgeline present in every tilted grid. The maximum branch length grid of the non-tilted terrain model is masked by the combined binary: if a cell in the combined grid has a value greater than a specified threshold [0…8], minimal shifting has occurred and the cell inherits the value of the corresponding cell in the maximum branch length grid derived from the non-tilted terrain model. If a cell has a value

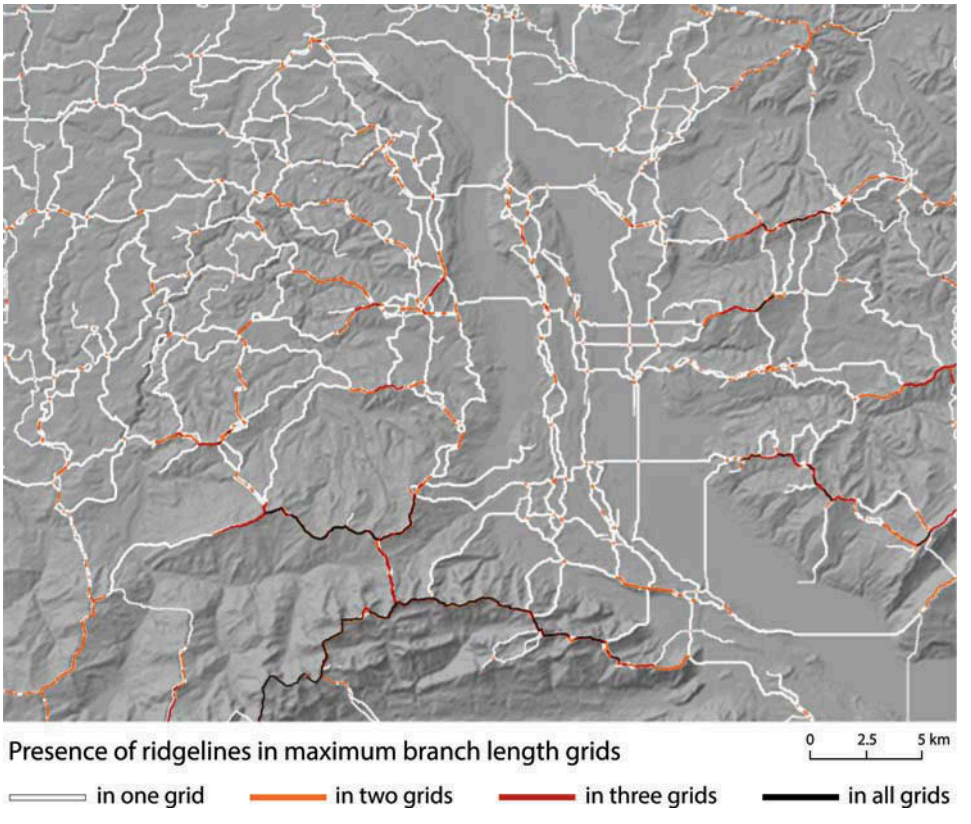

Figure 7. Ridgeline networks derived from tilting a terrain model in the four cardinal directions ($\gamma = 10\%$). The maximum branch length grids have been combined and overlaid on top of standard analytical shading. Colors represent the number of overlaps between the grids: white ridgelines are present in only one grid, indicating they experience maximum shifting during the tilting process; black ridgelines are present in all four grids, indicating they are the most stable ridgelines.

less than the threshold, excessive shifting of an unstable ridgeline has occurred and it is assigned a 0 value. The final grid is a filtered maximum branch length grid containing only stable ridgelines. The effectiveness of this technique in selecting prominent ridgelines, particularly in landscapes characterized by relatively flat terrain, is discussed further in the Evaluation and results section.

3.5. *Extracting terrain skeletal lines*

Extracting the ridgelines and valley lines from the maximum branch length and flow accumulation grids by vectorizing them is the second step for generating the diffusion curves. The maximum branch length and flow accumulation grids are converted to binary grids based on a user-defined threshold value. The threshold value is chosen according to the level of line detail desired by the user. Pixel values above the threshold are assigned a value of 1 and pixel values below the threshold are assigned a value of 0.

Two morphological operations are applied to the binary image. First, an iterative thinning algorithm (Lam *et al.* 1992, p. 879) converts the image to a skeleton by reducing lines to minimally connected strokes, one pixel thick (Haralick and Shapiro 1992, pp. 170–171). The second morphological operation, applied to the image skeleton, is an algorithm that locates branch points (Kong and Rosenfeld 1996, pp. 104–105), which identify the confluences of ridgelines or valley lines. The morphological operations are carried out using MATLAB's bwmorph function. Beginning at the branch points, a tracing algorithm converts the binary grid lines to vector lines (Figure 5c).

3.6. *Generalization of ridgelines*

Applying a graph analysis to a network of ridgelines generalizes line geometry and filters out short, unimportant ridgelines before the illumination adjustment. A graph is a series of vertices connected by edges. An undirected graph is constructed from the skeletal lines: ridgelines and valley lines are edges and vertices are located where lines converge. Generally, each vertex has degree three, meaning three edges connect to every vertex. The graph is without loops – no edge connects a vertex to itself – and there are no duplicate edges.

Short leaf edges – edges that are only connected on one side to the graph – are removed with a graph analysis algorithm. The result of the algorithm applied on a schematic ridgeline network is shown in Figure 8.

The algorithm is applied iteratively on the graph until there are no edges shorter than a designated threshold. On each iteration, the algorithm first locates the shortest leaf edge in the graph (Figure 8a) and then removes the edge if it is shorter than a user-defined threshold (Figure 8b). Once the edge is removed, the vertex it was connected to becomes degree two and is also removed from the graph structure (Figure 8c). The two remaining edges that shared the removed vertex are connected to form one new edge, which replaces the two original, separate edges (Figure 8d). Connecting and replacing the two original edges is necessary because the original edges may be shorter than the threshold and would also be removed, but the new combined edge may be longer and will remain in the graph structure. The graph analysis serves as a means to adjust the level of generalization to the map scale of the resulting shading image.

Additionally, a line simplification algorithm, such as the Douglas-Peucker simplification algorithm (Douglas and Peucker 1973), may be applied to the ridgelines and valley lines to simplify the diffusion curve geometry (Figure 9).

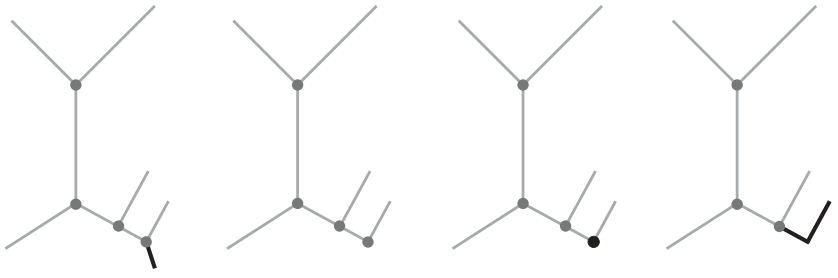

Figure 8. Graph analysis for ridgeline simplification. (a) Shortest leaf edge is identified. (b) It is removed. (c) Vertex with degree two is removed. (d) The two remaining edges are connected to form a new edge that replaces the original two edges.

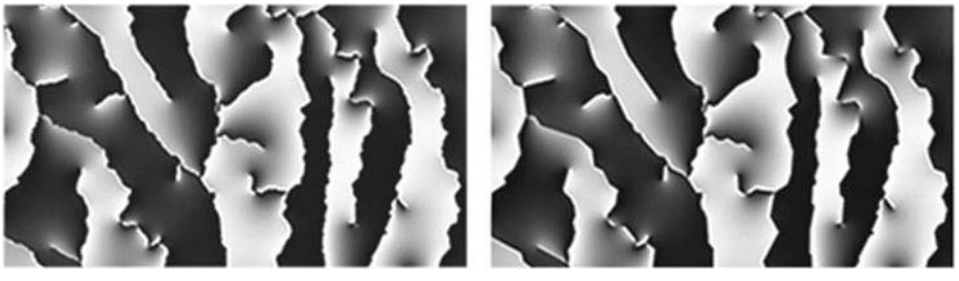

Figure 9. Diffusion curve shading without line simplification (left) and with line simplification (right).

3.7. *Illumination adjustment based on skeletal lines*

Local variations in the direction of illumination are determined by the spatial orientation of a ridge or valley. Similar to the method presented by Brassel (1974), the direction of illumination is locally adjusted for each skeletal line according to three variables:

(1) Standard direction of illumination, D_{st} $[0\ldots2\pi]$
(2) Maximum deviation of illumination, D_{max} $[0\ldots\frac{\pi}{2}]$
(3) Aspect of a ridgeline or valley line, β $[0\ldots2\pi]$

The standard direction of illumination (D_{st}) and the maximum deviation of illumination (D_{max}) are specified by the user. D_{max} is the maximum angle the adjusted illumination direction is allowed to deviate from the standard direction of illumination.

Aspect (β) is perpendicular to the orientation of each line segment. The difference (k) between the standard direction of illumination and aspect is computed: $k = D_{st} - \beta$. If $k \leq 0, k = k + \pi$. For $k < \frac{\pi}{2}$, the deviation of the illumination direction (D) from the standard direction of illumination for a ridge or valley is $D = \frac{-D_{max}}{\pi/2} \times k$. For $k \geq \frac{\pi}{2}$, $D = \frac{-D_{max}}{\pi/2} \times k + 2D_{max}$. The adjusted illumination direction for a ridge or valley is equal to $D_{st} + D$.

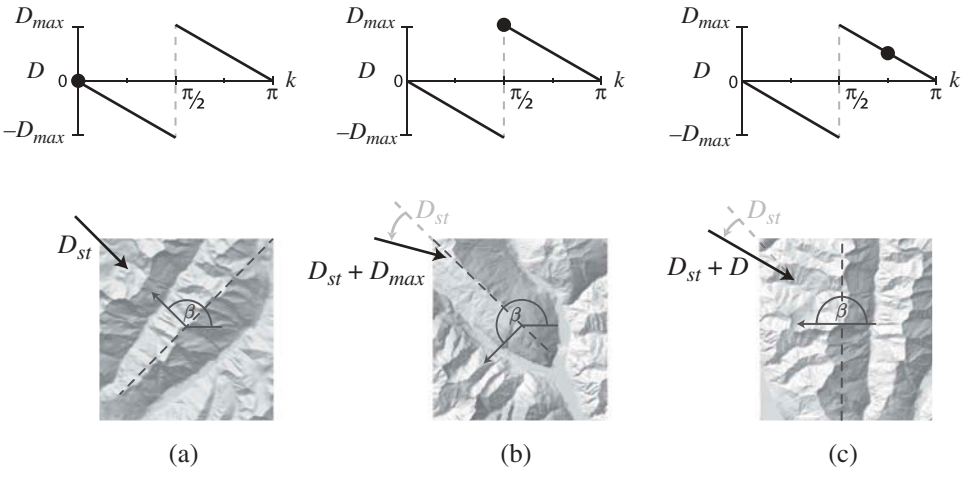

Figure 10. Illumination adjustment method. (a) Northeast-trending ridge receives no adjustment; (b) northwest-trending ridge receives maximum adjustment; (c) north-south-trending ridge receives moderate adjustment. The vertical axis represents the deviation (D) of the illumination direction from the standard direction of illumination (D_{st}). The horizontal axis is the difference (k) between D_{st} and the direction perpendicular to the line segment (β).

Figure 10, a graphical representation of the illumination adjustment method, illustrates how the illumination direction is adjusted for sample ridgelines trending in (a) northeast, (b) northwest, and (c) north-south directions. For a northeast-trending ridge, $k = 0$ and there is no adjustment of the illumination (Figure 10a). In this case, the standard direction of illumination is already striking the ridgeline in an optimal position. For a ridge or valley that is parallel to the standard direction of illumination, $k = \frac{\pi}{2}$ and the deviation (D) equals the maximum deviation ($\pm D_{max}$) (Figure 10b). For a north-south-trending ridge, $k = \frac{D_{max}}{2}$ and there is a moderate adjustment to the illumination direction (Figure 10c).

The aspect and the adjusted illumination directions calculated from non-simplified ridgeline and valley line segments are highly variable (Figure 11a). To reduce the variability of adjusted illumination directions, a line simplification algorithm, such as the Douglas-Peucker simplification algorithm (Douglas and Peucker 1973), can be applied to vectorized ridgelines and valley lines (Figure 11b and c). Simplifying the line geometry for computing the adjusted illumination results in more regular gray values along ridges and valleys.

Gray values assigned to the left and right sides of the diffusion curves are calculated using the adjusted illumination directions and simplified line geometry. Aspect-based shading (Moellering and Kimerling 1990), which accentuates the difference between shaded and illuminated sides of ridgelines and valley lines, is used to compute gray values: $g_{asp} = \frac{\cos(\alpha)+1}{2}$ where $g_{asp}[0 \ldots 1]$ is the gray value and α is the difference between the direction perpendicular to the line segment (β) and the azimuth of the adjusted illumination source $(D_{st} + D)$. Multiplying g_{asp} by 255 determines the gray value assigned to the diffusion curve. Jeschke *et al.*'s (2009) diffusion curve algorithm creates a shaded image from the gray values and diffusion curves.

The adjusted illumination method presented is based on Brassel's (1974) method. However, Brassel manually digitized the ridgelines and valley lines, whereas we have automated the digitizing process. In Brassel's method, the illumination directions, not the

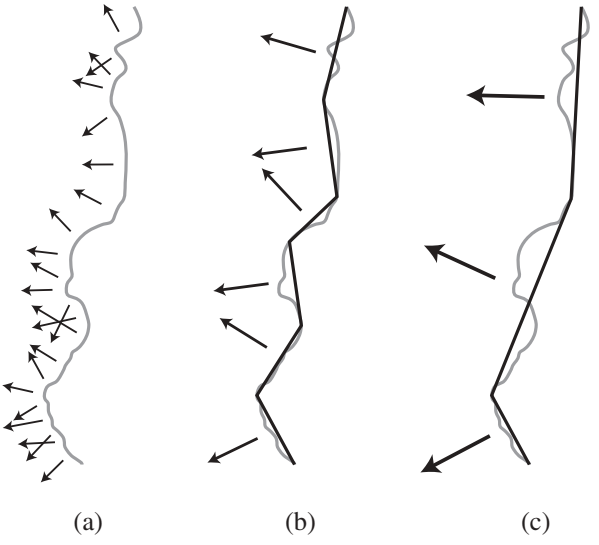

Figure 11. Douglas-Peucker line simplification for reducing the variability of adjusted illumination directions. (a) Aspect calculated from original line geometry. (b) Aspect calculated from line geometry simplified with low tolerance. (c) Aspect calculated from line geometry simplified with higher tolerance.

brightness values, are diffused across a geographic space. The light direction is adjusted by applying a model different from what Brassel used.

3.8. *Valley floor identification*

One of the primary design principles of Swiss-style relief shading is the placement of a bright gray tone in flat areas, such as valley floors, to visually connect adjacent mountain slopes (Imhof 1982). Valley floors, defined as relatively broad, flat regions within a valley, are detected using a seed fill algorithm (Heckbert 1990) based on the work of Straumann and Purves (2008). Our seed fill algorithm requires two inputs: (1) a terrain model, and (2) a stream network.

A flow accumulation grid is calculated from a terrain model as described in Section 3.3.1. Imposing a channel initiation threshold value on the flow accumulation grid produces a stream network raster. Stream cells are used as seed points for the seed fill algorithm. Beginning at the seed points, the algorithm tests whether the vertical difference between a seed cell and a neighboring non-seed cell is less than a specified gradient threshold. If the condition is met, the non-seed cell belongs to the valley floor and is filled. Cells neighboring filled cells are queried and filled in the same manner. Cells that have not been identified as valley floor cells, but are neighbored by at least four filled cells are filled to reduce patchiness. The seed fill algorithm is run iteratively until no new valley floor cells are detected. The result of the seed fill algorithm is an image that is overlaid on top of the diffusion curve shading and analytical relief shading as a mask for the valley floors.

3.9. *Software used*

Our method combines multiple methods, processes, and software that operate successively on a digital terrain model. The maximum branch length algorithm is implemented in

Whitebox Geospatial Analysis Tools (GAT) (Lindsay 2009), an extensible open-source GIS and remote sensing software package developed at the University of Guelph Centre for Hydrogeomatics. Using Python programming language, we wrote scripts for Whitebox GAT that applies the tilting method to a terrain model. Flow accumulation and stream network grids are calculated using the Flow Accumulation and Raster Calculator tools in Esri's ArcGIS software. Ridgelines and valley lines are converted to skeletal lines and branch points are located with MATLAB's bwmorph function. We trace skeletal lines with a custom algorithm in MATLAB. The graph analysis, local adjustment of illumination, and simplification of ridgeline and valley line geometry are executed with a custom Java application. We use the open-source JGraphT Java library for the graph analysis and manipulation (Naveh 2011). Open-source diffusion curve software developed by Jeschke *et al.* (2009) renders the final shaded image. We wrote the seed fill algorithm for detecting valley floors in MATLAB. Adobe Photoshop CS6 is used to overlay the diffusion curve shading on top of the analytical relief shading and mask the valley floors with the output from the seed fill algorithm.

4. Evaluation and results

Three study sites with different terrain characteristics were chosen to assess the feasibility and effectiveness of our method: (1) alpine terrain in southern Switzerland with an altitude difference greater than 3,000 meters; (2) pre-alpine terrain with hilly topography in Switzerland; and (3) a section of the Central Coast Range, Oregon, USA with a dense and complex drainage pattern. For the two test sites in Switzerland, we used the DHM25 terrain model from the Federal Office of Topography swisstopo with 25-meter resolution. For the Oregon study site, we used 10-meter resolution National Elevation Data provided by the U.S. Geological Survey. For all three sites, the relief shading generated with diffusion curve shading and locally adjusted illumination directions better highlights major landforms while still showing smaller details in each of the three sites (Figures 12–14). Major mountain ridges are emphasized with increased contrast between bright, illuminated slopes and dark, shadowed slopes. Locally shaded and illuminated slopes provide better structure to the terrain, thereby improving the aesthetic quality and helping users distinguish major features. Based on the three study sites, we determined the optimal standard direction of illumination (D_{st}) to be from the west-northwest at 160° with a preferred maximum deviation angle (D_{max}) of 30°. For all three sites, the Douglas-Peucker simplification algorithm was used to simplify both the diffusion curve geometry for the final diffusion curve shading and the line geometry used to compute the adjusted illumination.

4.1. Alpine terrain

Ticino, the southernmost canton of Switzerland, is located in the central Alps. The high, sharply defined peaks and deep valleys dominating the steep mountainous landscape make Ticino an ideal study site for demonstrating effective relief shading. Pizzo Erra (Figure 2), the highest point in the mountain ridge located north and slightly west of center in Figures 1 and 12, is a particularly interesting feature for evaluating relief shading methods because it is oriented parallel to the standard direction of illumination. Since Pizzo Erra is illuminated from a direction parallel to its ridge in standard analytical relief shading, the peak appears flatter than its actual appearance in the natural landscape. Ticino was also chosen because a manual relief shading reference

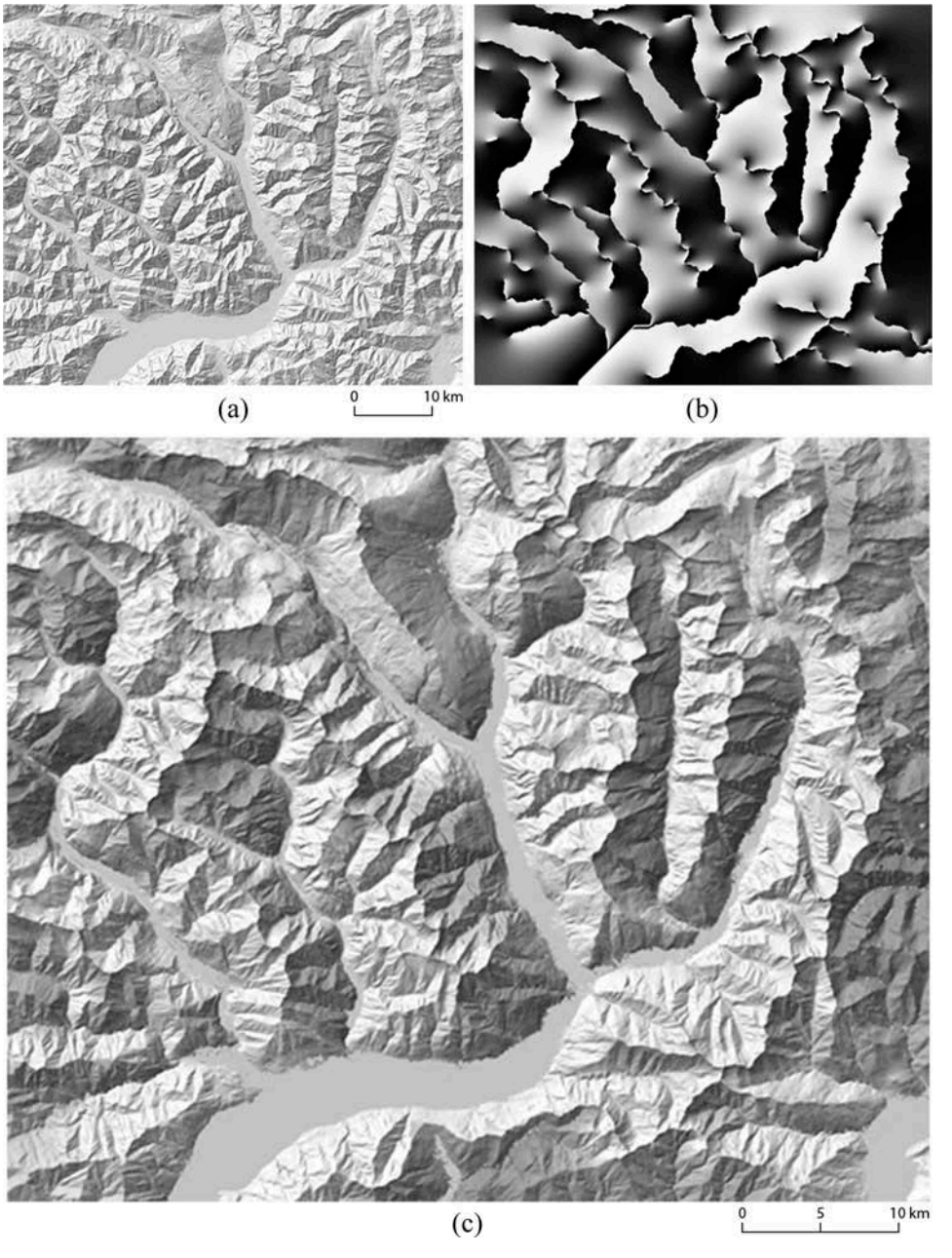

Figure 12. Alpine terrain results. (a) Standard analytical relief shading. (b) Diffusion curve shading. (c) Diffusion relief shading (combination of analytical shading and diffusion curve shading).

image, drawn by Imhof and Leuzinger in 1963 (Figure 1), can be used for comparison. Figure 12 shows (a) the analytical relief shading; (b) the diffusion curve shading generated with our method; and (c) the final relief shading produced by overlaying the diffusion curve shading on top of the analytical relief shading. In the final relief

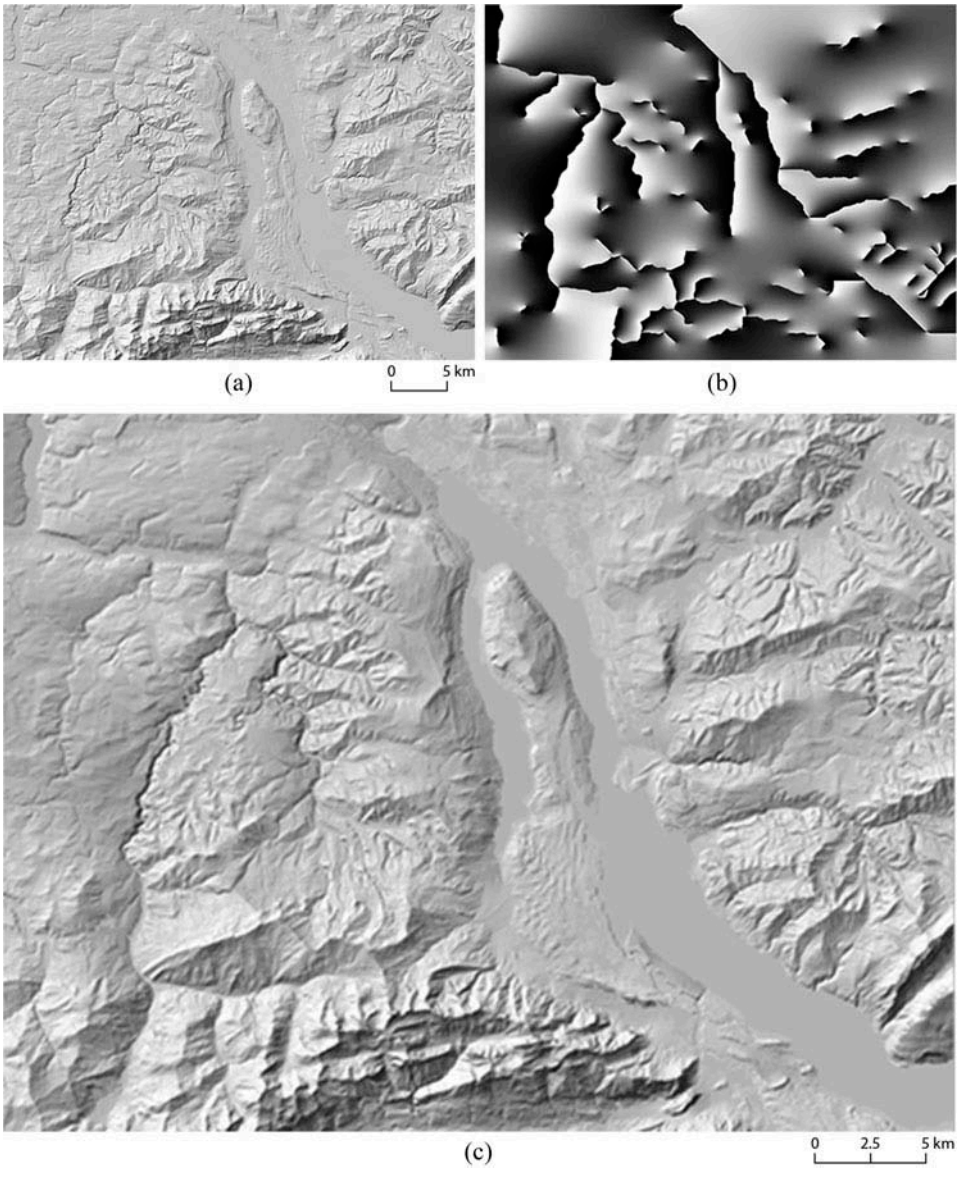

Figure 13. Pre-alpine terrain results. (a) Standard analytical relief shading. (b) Diffusion curve shading. (c) Diffusion relief shading (combination of analytical shading and diffusion curve shading).

shading, Pizzo Erra is locally illuminated from a more westerly direction, which accentuates the ridge and makes it appear more realistic. When comparing Figures 1 and 12, it is evident that the combination of standard shading and diffusion curve shading closely matches the visual quality of manual relief shading. Major landforms are more clearly visible because mountain ridges are structured in distinct shaded and

illuminated sides, and small details of the standard shading are still visible in the diffusion relief shading.

4.2. Pre-alpine terrain

The Gürbe Valley and the surrounding Prealps region in Switzerland were chosen as a study site due to their hilly relief with flat areas. Flat relief poses a significant challenge to creating effective, descriptive shading because transitions between illuminated and shaded slopes are smooth. Due to the flatter terrain, mountain passes, and rounded hills in the Gürbe Valley, the maximum branch length algorithm initially identified ridgelines that resulted in visually disturbing, unnatural interruptions in the diffusion curve rendering. The tilting and filtering process, explained in Section 3.4, was applied to the region, which retained significant ridgelines and successfully removed problematic ridgelines. A 10% elevation grade for γ produced optimal results for this study site (see Figure 7). The result of the diffusion relief shading is shown in Figure 13. The diffusion relief shading better highlights select terrain structures and creates a more descriptive and attractive image. However, the diffusion relief shading effect is not as strong as in the alpine example (Figure 12).

4.3. Terrain with complex drainage network

The third study site is a section of the Central Coast Range in northwest Oregon. The terrain is steep with defined ridges, but has generally low relief. There are fewer prominent peaks than in the Swiss Alps and the dense drainage network makes it difficult to define major terrain features. Ridges and valleys are difficult to identify. The standard analytical shading portrays the dense and intricate drainage patterns poorly. Results of the diffusion relief shading, shown in Figure 14, show improvement in terrain structure visualization. Discrete landforms are emphasized while smaller topographic details,

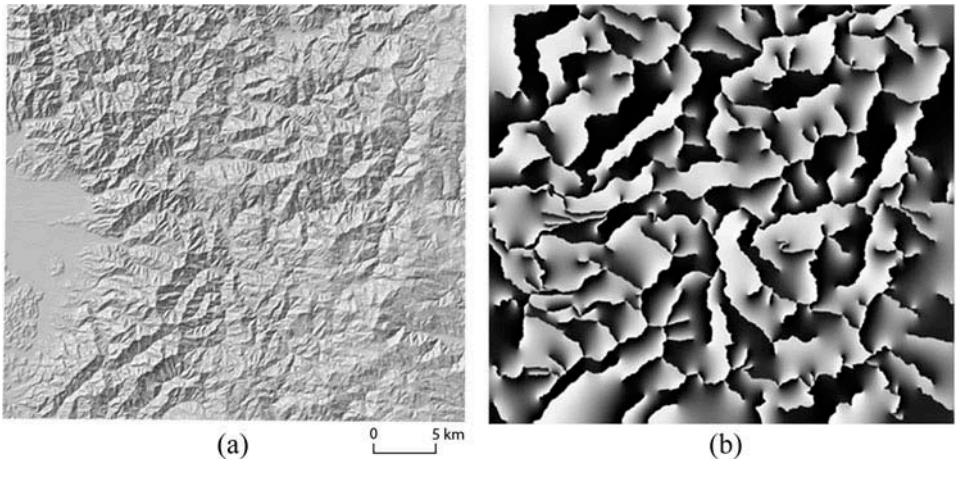

Figure 14. Results for terrain with complex drainage network. (a) Standard analytical relief shading. (b) Diffusion curve shading. (c) Diffusion relief shading (combination of analytical shading and diffusion curve shading).

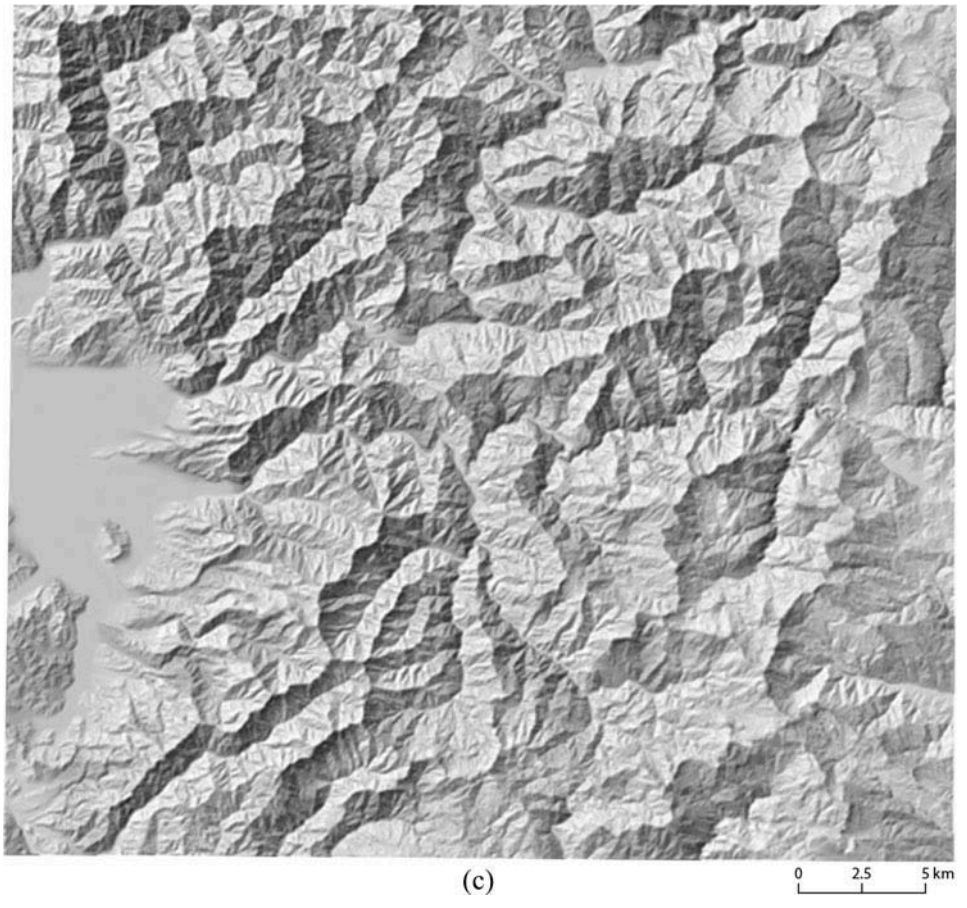

Figure 14. (Continued).

although still present, are more subdued. Illuminated and shaded slopes make it easier to distinguish the various hydrographic flow patterns in the complex terrain.

5. Conclusion

The presented automated digital method for creating relief shading simulates the cartographic design techniques and principles associated with Swiss-style manual relief shading. Our method is a combination of multiple methods that automate the local adaptation of illumination in relief shading using a diffusion curve rendering algorithm.

The diffusion relief shading best highlights major landforms in terrain characterized by sharp, clearly defined ridges and valleys, as can be seen in Figures 12 and 14. The benefits of the diffusion relief shading are less pronounced in flatter topography and regions with rounded hills (Figure 13). For this type of terrain, however, the tilting method effectively removes irrelevant or visually disturbing ridgelines that do not fit the natural characteristics of the landscape. For each study site chosen to test the feasibility of our method, the diffusion relief shading enhanced the analytical shading to produce

relief shading that depicts major landforms more clearly and is more aesthetically pleasing.

Our method presents an alternative to other filter-based generalization approaches, which typically smooth ridges (Guilbert *et al.* 2014). However, sharp terrain structures need to be retained to illustrate the characteristic shapes and structure of mountainous terrain. With our method, the user can adjust the level of detail in the shaded relief by choosing parameters for line geometry simplification and graph-based simplification. These approaches retain the sharp features of mountainous areas that are often eliminated or smoothed with other generalization techniques.

There are some limitations to our method. The spatial extent of the terrain model can impact the result of the maximum branch length algorithm. If the confluence of flow paths is located beyond the extent of the terrain model, the maximum branch length value may be underestimated. Runtime for the various processes is also influenced by the extent of the terrain and the topography of a selected site. The vectorization, graph analysis, illumination adjustment, and diffusion curve algorithms all have fast completion rates ranging from a fraction of a second to a few seconds. However, the time to run the maximum branch length algorithm is highly variable, taking anywhere between several minutes – for a small terrain extent with a simple ridge network – to several hours for a larger extent. The tilting process for relatively flat terrain requires the maximum branch length algorithm to be run up to eight times, one for each cardinal and intercardinal direction, and is often a time-consuming task requiring multiple hours for computation. We believe the maximum branch length algorithm computation could be accelerated, but to do so requires further research. Although the seed fill algorithm is able to identify the majority of the valley floor, results for all three sites contained unwanted artifacts in valley floors, such as patches, which required correcting with image editing software to make a suitable mask for the final diffusion relief shading image.

Evaluating the results of shading methods is challenging. In an attempt to evaluate results quantitatively, we computed the per-pixel difference in gray values between the manual relief shading (Figure 1) and the diffusion relief shading (Figure 12c), as well as the standard analytical shading (Figure 12a). New grayscale images showing the difference between the shading images were produced. There was less variation between the manual and diffusion relief shadings than between the manual and standard analytical shadings. However, this method of evaluation has several flaws. First, the quality of manual relief shading varies with the skill, experience, and individual style of the relief artist (Leonowicz *et al.* 2010a). Second, the evaluation is visual, not quantitative, by nature. We believe that a visual assessment remains the most practical and reliable method for evaluating the results and effectiveness of relief shading methods.

Future developments could be made to incorporate hypsometric tinting or colors that are modulated by elevation and exposure to illumination (Jenny and Hurni 2006). The numerous software applications we use are a pragmatic choice for the development of our method, but they should be integrated into a user-friendly interface to make our method more accessible to a larger audience. Our method also requires numerous parameters for various procedures. Choosing parameter values is largely subjective and relies heavily on map scale, terrain characteristics, and intended level of detail in the final diffusion relief shading image. More research should be conducted to find recommendable values. Additionally, it would be interesting to explore whether highlighting major landforms with locally adjusted illumination directions impacts the relief inversion effect (Bernabé Poveda and Çöltekin 2014). It is our hope that the results

presented in this article inspire cartographers to continue improving the quality of analytical relief shading.

Acknowledgements

The authors would like to thank William McNulty of Google for his support and the following organizations for funding assistance: Google, Oregon State University, the Alpha Chapter of Phi Beta Kappa at the University of Colorado at Boulder, the Association of American Geographers Cartography Specialty Group, and the International Cartographic Association Commission on Mountain Cartography. The authors would also like to thank Tom Patterson at the National Park Service for his valuable insight and assistance in this research.

References

Bernabé Poveda, M.A. and Çöltekin, A., 2014. Prevalence of the terrain reversal effect in satellite imagery. *International Journal of Digital Earth (ahead-of-print)*, 1–24. doi:10.1080/17538947.2014.942714

Bezerra, H., *et al*., 2010. Diffusion constraints for vector graphics. *In*: M. McGuire, P. Ascente, and S. Spencer, eds. *NPAR* 2010: *proceedings of the 8th international symposium on non-photorealistic animation and rendering*, 7–10 June, Annecy. New York, NY: ACM, 35–42.

Boyé, S., Barla, P., and Guennebaud, G., 2012. A vectorial solver for free-form vector gradients. *ACM Transactions on Graphics*, 31 (6), 173. doi:10.1145/2366145.2366192

Brassel, K., 1974. A model for automatic hill-shading. *The American Cartographer*, 1 (1), 15–27. doi:10.1559/152304074784107818

Collier, P., Forrest, D., and Pearson, A., 2003. The representation of topographic information on maps: the depiction of relief. *The Cartographic Journal*, 40 (1), 17–26. doi:10.1179/000870403235002033

Douglas, D.H. and Peucker, T.K., 1973. Algorithms for the reduction of the number of points required to represent a digitized line or its caricature. *Cartographica: the International Journal for Geographic Information and Geovisualization*, 10 (2), 112–122. doi:10.3138/FM57-6770-U75U-7727

Finch, M., Snyder, J., and Hoppe, H., 2011. Freeform vector graphics with controlled thin-plate splines. *ACM Transactions on Graphics*, 30 (6), 166. doi:10.1145/2070781.2024200

Geisthövel, R., 2013. Towards automating Swiss style rock depiction (oral presentation). *In*: *26th International Cartographic Conference*, 25–30 August, Dresden.

Guilbert, E., Gaffuri, J., and Jenny, B., 2014. Terrain generalisation. *In*: D. Burghardt, C. Duchêne, and W. Mackaness, eds. *Abstracting geographic information in a data rich world*. New York, NY: Springer, 227–258.

Haralick, R.M. and Shapiro, L.G., 1992. *Computer and robot vision*, Vol. I. Boston, MA: Addison-Wesley.

Heckbert, P.S., 1990. A seed fill algorithm. *In*: A.S. Glassner, ed. *Graphics Gems*. San Diego, CA: Academic Press Professional, 275–277.

Hobbs, K.F., 1999. An investigation of RGB multi-band shading for relief visualisation. *International Journal of Applied Earth Observation and Geoinformation*, 1 (3–4), 181–186. doi:10.1016/S0303-2434(99)85011-9

Hodgkiss, A.G., 1981. *Understanding maps: a systematic history of their use and development*. Folkestone: Dawson.

Hurni, L., 2008. Cartographic mountain relief presentation. *In*: L. Hurni and K. Kriz, eds. *Mountain mapping and visualisation: proceedings of the 6th ICA mountain cartography workshop*, 11–15 February, Lenk. Zurich: ETH Zurich, 85–91.

Imhof, E., 1982. *Cartographic relief presentation*. Berlin: de Gruyter.

Jenny, B., 2001. An interactive approach to analytical relief shading. *Cartographica: The International Journal for Geographic Information and Geovisualization*, 38 (1), 67–75. doi:10.3138/F722-0825-3142-HW05

Jenny, B. and Hurni, L., 2006. Swiss-style colour relief shading modulated by elevation and by exposure to illumination. *The Cartographic Journal*, 43 (3), 198–207. doi:10.1179/000870406X158164

Jenny, B., Hutzler, E., and Hurni, L., 2010. Scree representation on topographic maps. *The Cartographic Journal*, 47 (2), 141–149. doi:10.1179/000870409X12525737905006

Jeschke, S., Cline, D., and Wonka, P., 2009. A GPU Laplacian solver for diffusion curves and Poisson image editing. *ACM Transactions on Graphics*, 28 (5), 116. doi:10.1145/1618452.1618462

Jeschke, S., Cline, D., and Wonka, P., 2011. Estimating color and texture parameters for vector graphics. *Computer Graphics Forum*, 30 (2), 523–532. doi:10.1111/j.1467-8659.2011.01877.x

Karssen, A.J., 1982. Mask hill shading: a new method of relief representation. *ITC Journal*, 1982 (2), 160–169.

Keates, J.S., 1996. *Understanding maps*. 2nd ed. Harlow: Longman.

Kennelly, P.J., 2008. Terrain maps displaying hill-shading with curvature. *Geomorphology*, 102 (3–4), 567–577. doi:10.1016/j.geomorph.2008.05.046

Kennelly, P.J. and Stewart, A.J., 2006. A uniform sky illumination model to enhance shading of terrain and urban areas. *Cartography and Geographic Information Science*, 33 (1), 21–36. doi:10.1559/152304006777323118

Knowles, R. and Stowe, P.W.E., 1982. *Western Europe in maps: topographical map studies*. Harlow: Longman.

Kong, T.Y. and Rosenfeld, A., eds., 1996. *Topological algorithms for digital image processing*. Amsterdam: Elsevier.

Lam, L., Lee, S.-W., and Suen, C.Y., 1992. Thinning methodologies—A comprehensive survey. *IEEE Transactions on Pattern Analysis and Machine Intelligence*, 14 (9), 869–885. doi:10.1109/34.161346

Leonowicz, A.M., Jenny, B., and Hurni, L., 2010a. Automated reduction of visual complexity in small-scale relief shading. *Cartographica: The International Journal for Geographic Information and Geovisualization*, 45 (1), 64–74. doi:10.3138/carto.45.1.64

Leonowicz, A.M., Jenny, B., and Hurni, L., 2010b. Terrain sculptor: generalizing terrain models for relief shading. *Cartographic Perspectives*, 67, 51–60. doi:10.14714/CP67.114

Lindsay, J.B., 2009. Whitebox geospatial analysis tools. Department of Geography, University of Guelph. Available from: http://www.uoguelph.ca/~hydrogeo/Whitebox/download.shtml [Accessed February 2014].

Lindsay, J.B. and Seibert, J., 2013. Measuring the significance of a divide to local drainage patterns. *International Journal of Geographical Information Science*, 27 (7), 1453–1468. doi:10.1080/13658816.2012.705289

Loisios, D., Tzelepis, N., and Nakos, B., 2007. A methodology for creating analytical hill-shading by combining different lighting directions. *In*: *Proceedings of 23rd International Cartographic Conference* [online], 4–10 August, Moscow. LOC. Available from: http://icaci.org/files/documents/ICC_proceedings/ICC2007/html/Proceedings.htm [Accessed February 2014].

Mark, R., 1992. *A multidirectional, oblique-weighted, shaded-relief image of the Island of Hawaii* (Technical Report OF-92-422) [online]. U.S. Department of the Interior, U.S. Geological Survey. Available from: http://permanent.access.gpo.gov/lps53178/lps53178/pubs.usgs.gov/of/1992/of92-422/index.htm [Accessed June 2014].

Moellering, H. and Kimerling, J.A., 1990. A new digital slope-aspect display process. *Cartography and Geographic Information Systems*, 17 (2), 151–159. doi:10.1559/152304090783813853

Naveh, B., 2011. *JGraphT a free Java graph library* [online]. Available from: https://github.com/jgrapht/jgrapht [Accessed May 2014].

O'Callaghan, J.F. and Mark, D.M., 1984. The extraction of drainage networks from digital elevation data. *Computer Vision, Graphics, and Image Processing*, 28 (3), 323–344. doi:10.1016/S0734-189X(84)80011-0

Orzan, A., *et al*., 2008. Diffusion curves: a vector representation for smooth-shaded images. *ACM Transactions on Graphics (Proceedings of SIGGRAPH 2008)*, 27, 92.

Patterson, T., 2001. *Creating Swiss-style shaded relief in Photoshop* [online]. Available from: http://www.shadedrelief.com/shading/Swiss.html [Accessed June 2014].

Patterson, T. and Hermann, M., 2004. *Creating value-enhanced shaded relief in Photoshop* [online]. Available from: http://www.shadedrelief.com/value/value.html [Accessed June 2014].

Prechtel, N., 2000. Operational analytical hill shading within an advanced image processing system. *In*: M.F. Buchroithner, ed. *Proceedings of the 2nd workshop on high mountain cartography, Kartographische Bausteine*, Vol. 18, 29 March–2 April, Rudolfshütte. Dresden University of Technology, 85–98.

Ristow, W.W., 1975. Lithography and maps 1796–1850. *In*: D. Woodward, ed. *Five centuries of map printing*. Chicago, IL: University of Chicago Press, 77–112.

Straumann, R.K. and Purves, R.S., 2008. Delineation of valleys and valley floors. *In*: T.J. Cova, *et al*., eds. *Geographic information science: 5th international conference, GIScience 2008, Proceedings, lecture notes in computer science (5266)*, Park City, UT, 23–26 September. Berlin: Springer, 320–336.

Tufte, E.R., 1990. *Envisioning information*. Cheshire, CT: Graphics Press.

van de Gronde, J., 2010. *A high quality solver for diffusion curves*. Thesis. University of Groningen.

Veronesi, F. and Hurni, L., 2014. A GIS tool to increase the visual quality of relief shading by automatically changing the light direction. *Computers & Geosciences*, 74, 121–127.

Weibel, R., 1992. Models and experiments for adaptive computer-assisted terrain generalization. *Cartography and Geographic Information Systems*, 19 (3), 133–153. doi:10.1559/152304092783762317

Wiechel, H., 1878. Theorie und Darstellung der Beleuchtung von nicht gesetzmässig gebildeten Flächen mit Rücksicht auf die Bergzeichnung (in German). *Civilingenieur*, 24, 335–364.

Wilson, J.P. and Gallant, J.C., eds., 2000. *Terrain analysis: principles and applications*. New York, NY: John Wiley and Sons.

Yoeli, P., 1959. Relief shading. *Surveying and Mapping*, 19 (2), 229–232.

Yoeli, P., 1965. Analytical hill shading. *Surveying and Mapping*, 25 (4), 573–579.

Yoeli, P., 1966. Analytical hill shading and density. *Surveying and Mapping*, 26 (2), 253–259.

Yoeli, P., 1967. The mechanisation of analytical hill shading. *The Cartographic Journal*, 4 (2), 82–88. doi:10.1179/caj.1967.4.2.82